AD-A126 325 FIBER OPTIC MAGNETIC SENSOR RESEARCH(U) PHOENIX CORP 1/1
MCLEAN VA S J PETUCHOWSKI 28 FEB 83 N00014-82-C-2201

UNCLASSIFIED F/G 17/6 NL

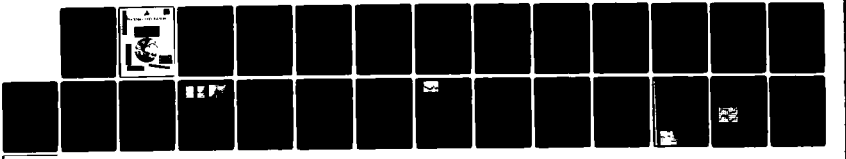

END
DATE FILMED
4-83
DTIC

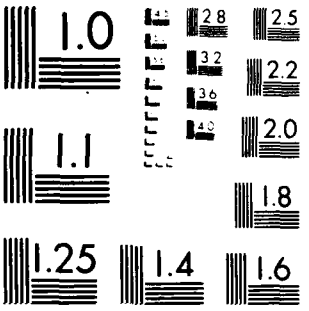

(13)

FIBER OPTIC MAGNETIC SENSOR RESEARCH

Final Report for the Period
May 21, 1982 - February 28, 1983

on

N00014-82-C-2201

for

U.S. Naval Research Laboratory
Washington, D.C.

by

Phoenix Corporation
1700 Old Meadow Road
McLean, Virginia 22102

TABLE OF CONTENTS

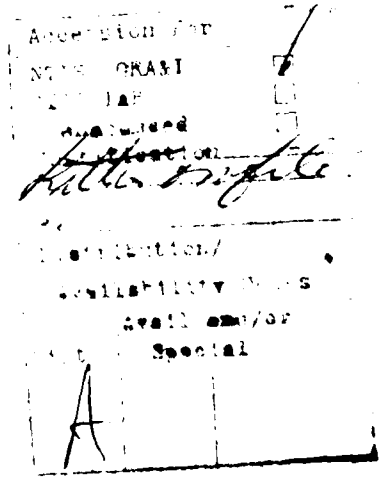

1. OVERVIEW

This report summarizes the research performed by the Phoenix Corporation under U. S. Naval Research Laboratory Contract No. N00014-82-C-2201 during the period May 21, 1982 to February 28, 1983. The basic goals of this research have entailed a continuation of research performed under a prior contract, N00014-81-C-2148, with the basic thrust lying in furthering the state of the art in the area of fiber optic magnetometers. This work was performed by Phoenix Corporation Staff Scientist, Dr. Samuel J. Petuchowski, on the premises of the Navel Research Laboratory, Washington, D. C.

2. MAGNETOMETRIC STUDIES

The direction of technological advance which will lead to the development of a deployable fiber-optic magnetic sensor has been brought into closer focus as a result of studies conducted under this contract. It is useful to categorize our work as comprised of the following constituent efforts:

A. Componentry and configuration of optical sensors in general;

B. Transductive componentry whereby a magnetic field effects a measurable change in a sensor system. This includes characterization and optimization of magnetostrictive materials;

C. Configuration of a magneto-sensitive material for specialized applications (tailoring of orientational characteristics, for example) for measurement of total field, vector field, field gradient, etc.;

D. Data acquisition techniques suited to the chosen transduction mechanism and the optical configuration and sensitivity/spectral-response requirements of the application.

We note that all the above efforts are system-related and must be addressed accordingly. Our summary of research highlights under the rubrics of the tasks set forth in the Statement of Work will be subsumed under the headings listed above.

A. Componentry and configuration of optical sensors in general

Experimental characterization of magnetometric configurations during the reporting period employed a Mach-Zehnder fiber interferometer which incorporated a single (transverse) -mode optical fiber path and a single (longitudinal and transverse) -mode diode laser source. A integral fiber optic magnetometer employing no bulk optical components was demonstrated for the first time under this contract. The laser source was a .83 μm GaAlAs laser supplied by Laser Diode Labs and "pigtailed" by the manufacturer to a single-mode ITT optical fiber. This technology has been developed at NRL in support of various FOSS (Fiber Optic Sensor System Program) efforts such as the hydrophone, fiber gyroscope, etc,; and the further progress in component fabrication (sources, fibers, couplers, detectors) and noise reduction will be of a "generic" nature common to the entire FOSS technology.

Several aspects of the optical technology were addressed under this contract:

1. Laser source frequency instability (or, equivalently, phase noise) has been identified as a major limitation to the sensitivity of interferometric sensors at low frequencies (see A. Dandridge, et al., Appl. Phys. Lett.37, 1980) as well as to coherent communications. The incorporation of a diode lasing medium in a three-mirror external cavity was shown to limit laser emission linewidth to less than 200 kHz. These experiments are described in Appendix C.

2. A scheme involving the demonstrated injection-locking capability of a diode laser as well as the narrow spectral feedback afforded by an atomic vapor filter was disclosed (Appendix A).

3. The sensitivity of fiber interferometers to thermal effects was investigated in some depth. The application of FOSS technology to point and distributed temperature sensors, of potentially great impact for the Navy, was demonstrated and is described in Appendices E and F. Preliminary proof of principle was conducted on the disclosure of a Michelson interferometric fiber optical point temperature sensor (Appendix B). The sensor has potential application to non-invasive and high-bandwidth temperature measurement in flames and biomedia.

4. An extension of interfreometric techniques to the sensitive measurement of small absorptions in a medium (for characterization of optical media or for trace detection, for example) was pursued, resulting in the demonstration, described in Appendix D, of a Fabry-Perot photothermal trace detection apparatus.

B. Transductive components

Given the current state of the art in materials technology, the use of magnetostriction in a suitable material coupled mechanically to an optical fiber, in order to modify the propagation of a light wave guided through the fiber, appears to be the most promising mechanism to allow magnetometrics to benefit from the known advantages of fiber sensor technology. These advantages include remote EMI-free deployment capability, the potential deployment of an array of multiple sensors sharing a single remote light source, and sensitivity enhancement for transduction schemes which scale with fiber length, since long fiber segments can be configured

in small volumes. This is not to say that fundamental physical considerations preclude the future development of a magneto-optical transduction mechanism at least as sensitive as the magnetostrictive scheme, if a suitable material is discovered.

Optimal magnetic field sensitivity of a magnetostrictive transduction scheme dictates the search for a material with maximal slope of induced strain vs.applied magnetic field, $\partial E/\partial H$, which implies a search for a material with a large saturation magnetostriction, λ_s, as well as one with magnetostrictive saturation achieved at a low value of external field. Both conditions appear likely to be met using a metallic glass material as opposed to a crystalline metal allow. This was borne out in studies in which lengths of fiber bonded to Metglas® (Allied Corp.) samples were incorporated as one arm of a fiber interferometric test setup. Induced optical phase shift was measured as a function of applied magnetic field.

Conclusions, in this regard, as of this writing:

1. The functional dependence of the magnetostrictive strain in a metallic glass vs. the applied field varies with many parameters. including:
    a. material composition;
    b. material thermal history including:
        (1) method of fabrication (splat-quenching or sputtering).
        (2) anneal temperature, duration, applied magnetic field or strain during anneal;
    c. geometry of magnetostrictive member;
    d. method of bonding fiber to magnetostrictive member;
    e. surface degradation to oxidation.

2. Research to date has only begun to provide a data base from which to infer preferred materials processing recipes and and to project achievable field sensitivities. The best $\partial E/\partial H$ achieved under this contract was 250 rad/Oe/M in a sample of Metglas 2601-SC annealed at 325°C under longitudinal tension and an obliquely directed magnetic field of 130 Oe for ~20 min. A systematic study in which different Metglas compositions will undergo different anneal procedures and will be bonded to fibers for measurement of E-H curves was initiated and will be carried out by Drs. Doon and Edelstein of the Naval Research Lab in collaboration with the

Optical Materials Section of the Optical Techniques Branch at NRL.

3. Data surveyed suggest that while λ_s, for a given material composition, is insensitive to thermal history, the "knee" (onset of saturation) can be manipulated by inducing a magnetic anisotropy through the field annealling process. It is our recommendation that significant effort be committed to developing a fundamental understanding of the physics underlying this phenomenolgy in order to define wisely a technological approach to the fiber magnetometer problem.

4. Hysteresis of B vs. H is a necessary concomitant of ferromagnetic materials. The lowest coercive forces in this class have indeed been found in annealed metallic glasses, however, even these are significant (~mOe) on the magnitude scale of low frequency fields to be detected in naval applications. Hysteretic behavior is documented in our data. The implication for a magnetometric application is that some scheme will be required to "erase" the field memory prior to each measurement so that the measured value of induced strain uniquely maps a value of applied field. This involves driving the material to reset from magnetostrictive saturation, and such a scheme was modeled experimentally and is described below in Section D.

C. Configuration of the magneto-sensitive material

Most of the magnetometer experiments during the reporting period were conducted using a linear sensor configuration: a 4-5-cm length of unjacketed optical fiber bonded along the center of a 1-cm-wide strip of splat-quenched metallic glass. Considerations of symmetry dictate that the strain induced along the fiber axis in the presence of an axial bias field is linear in the external axial field and dependent on the transverse fields only in second order. Any observed transverse-field effect was down by greater than 40dB, which was the resolution to which the orthogonality of the applied fields could be gauged with a Hall-effect probe.

Preliminary investigation was performed on samples of fiber on which metallic glass had been deposited by rapid sputtering from a conical Metglas target by NRL researchers of the Magnetics Branch. Much work remains to be done in developing this technology since direct sputtering onto the fiber induced large scattering losses in the fiber and caused it to be exceedingly brittle. One promising tack appears to accrue from

sputtering over fiber pre-jacketed with a layer of aluminum. A sample sputtered while an electric current was passed through the aluminum under-jacket remains to be evaluated.

D. Data acquisition techniques

The challenge unique to magnetometry among FOSS sensor applications is the requirement of effective DC detection capability. The fact that various processes contributing to sensor noise and degrading sensitivity, by causing excursions of the interferometer operating point from quadrature, all manifest 1/f - law dependence suggests that some means of noise compensation must be implemented.

A scheme utilizing two optical polarizations within a fiber interferometer was advanced by Dr. Petuchowski and might become viable as polarization-maintaining optical fibers become available.

Other studies invoked the principle of an applied AC magnetic bias and the net quadratic response of the material. To test such data acquisition techniques, a mock-up has been configured in which the symmetric material response is simulated by a piezoelectric fiber stretching cylinder driven by a quadratic waveform. By sampling over a short gate within a large total optical phase excursion amplitude each cycle, behavior similar to that of a fluxgate magnetometer can be simulated. This suggests the possiblity of achieving magnetostrictive saturation once per half cycle of the AC bias field, thereby addressing the hysteresis problem (since magnetostrictive 'memory' would be erased twice per cycle). The circuitry for this scheme has been provided to the technical monitor of this contract.

In order to measure the noise characteristics of this scheme at very low frequencies, a desktop computer and Fourier-transform spectrum analyser have been interfaced to the mock-up, with documentation located at NRL.

3. SUMMARY

In the course of the research performed under this contract, we have made substantial progress in several parallel aspects of the development of a fiber-optic magnetometer. The optical aspects of the technology are advancing apace and are adequate to many foreseen applications, pending further progress into the understanding and application of magnetostrictive materials. A systematic survey of the properties of magnetostrictive metallic glasses, especially as bonded to optical fibers, has been shown to be a high priority of this effort and has been initiated by the Naval Research Laboratory.

4. PUBLICATIONS AND PRESENTATIONS

S. J. Petuchowski, R. O. Miles, A. Dandridge and T. G. Giallorenzi, "A Fox-Smith Diode Laser Source- Line Narrowing and Sensor Applications", presented at the Topical Meeting on Optical Fiber Communications, Phoenix, AZ, April, 1982.

S. J. Petuchowski, G. S. Maurer and Luise Schuetz, "Fiber Optic Thermal Sensors", presented at the 1982 Tri-Service FOSS Workshop, Ft. Eustis, VA, October, 1982.

S. J. Petuchowski, G. H. Sigel and T. G. Giallorenzi, "Single-Mode Fibre Point and Extended Termperature Sensors", Electronics Letters 18, 814, 1982.

A. J. Campillo, S. J. Petuchowski, C. C. Davis and H-B. Lin, "F[illegible]-Perot Photthermal Trace Detection", Appl. Phys. Lett. 41, 327, 1[illegible]

5. SCIENTIFIC PERSONNEL ASSOCIATED WITH CONTRACT

Samuel J. Petuchowski, Staff Scientist

APPENDIX A

RECORD AND DISCLOSURE OF INVENTION
NAVSO 5870/35 (REV. 6-73)
S/N 0104-LF-908-0198

DEPARTMENT OF THE NAVY
OFFICE OF NAVAL RESEARCH
ARLINGTON, VA. 22217

INSTRUCTIONS. A Navy employee or an employee of a Navy contractor should use this form when submitting an invention disclosure to the Department of the Navy. Original and two copies should be printed or typed and forwarded to the Navy Patent representative in the area or directly to the Office of Naval Research at the above address. Where space on form is inadequate, enter "see attached page", identify item by number and use plain pages as needed. When completely executed, this form becomes an important legal document useful in proving priority of invention.

FOR USE BY NAVY PATENT ACTIVITY

PATENT ACTIVITY (Name)	NAVY CASE NO.
	66,933
DATE OF [illegible]	[illegible]
12 Aug, 1982	

PART I. RECORD OF INVENTION

1. INVENTOR(S)	ADDRESS	POSITION TITLE	EMPLOYER (Activity & Code No., or Company & address)
Samuel J. Petuchowski	NRL B12, R201 (202) 767-2870	Research Physicist	Phoenix Corporation, McLean, VA

2. DESCRIPTIVE TITLE OF INVENTION (Disclose details of invention on Part II on reverse)

Self-Injection Locked, Lamb-Dip Stabilized Diode Laser

RECOMMENDED SECURITY CLASSIFICATION ON INVENTION DISCLOSURE

Unclassified

3. CONCEPTION, INITIAL RECORDS AND RESULTS OF FIRST MODEL

a. EARLIEST DATE AND PLACE INVENTION WAS CONCEIVED (Identify persons and records to support date and place)

June 9, 1982 - recorded in lab notebook, discussed with A. Dandridge and Lew Goldberg in NRL B12/R356

b. DATE AND PRESENT LOCATION OF FIRST SKETCH, DRAWING OR PHOTO AND FIRST WRITTEN DESCRIPTION (Such as notebook entries, etc.)

Lab notebook of inventor, NRL B12/R201; other notes at same location

c. DATE AND PLACE OF COMPLETION OF FIRST OPERATING MODEL OR FULL SIZE DEVICE AND ITS PRESENT LOCATION

None

d. DATE AND PLACE OF FIRST TEST OR OPERATION AND THE RESULTS (Give name and address of witnesses, and present location of records)

None

4. OTHER RECORDS (Notebook entries, descriptions, reports, drawings, etc.)

IDENTIFICATION	DATE OF DOCUMENT	PRESENT LOCATION
None		

5. OTHER INDIVIDUALS TO WHOM INVENTION WAS DISCLOSED

NAME	ACTIVITY OR COMPANY INDIVIDUAL REPRESENTS	DATE DISCLOSED	TYPE (Oral or written disclosure)
A. Dandridge	John Carrol U	6/9/82	Oral
L. Goldberg	Naval Research Lab	6/9/82	Oral

6. DATE AND PLACE OF OTHER TESTS OR OPERATIONS, AND THE RESULTS (Give name and address of witnesses and identify present location of records)

None

NAVSO 5870/35 (REV. 6-73)
S/N 0104-LF-908-0198

DEPARTMENT OF THE NAVY
OFFICE OF NAVAL RESEARCH
ARLINGTON, VA. 22217

APPENDIX B

INSTRUCTIONS. A Navy employee or an employee of a Navy contractor should use this form when submitting an invention disclosure to the Department of the Navy. Original and two copies should be printed or typed and forwarded to the Navy Patent representative in the area or directly to the Office of Naval Research at the above address. Where space on form is inadequate, enter "see attached page", identify item by number and use plain pages as needed. When completely executed, this form becomes an important legal document useful in proving priority of invention.

FOR USE BY NAVY PATENT ACTIVITY	
PATENT ACTIVITY (Name)	NAVY CASE NO. 67,201
DATE DISCLOSURE RECEIVED	LOCAL CASE NO

PART I. RECORD OF INVENTION

1. INVENTOR(S)	ADDRESS	POSITION TITLE	EMPLOYER (Activity & Code No., or Company & address)
Samuel J. Petuchowski	NRL Code 6570	Research Physicist	Phoenix Corp., McLean, VA
Thomas G. Giallorenzi	NRL Code 6500	Division Superintendent	NRL
	Tel. 767-2870		

2. DESCRIPTIVE TITLE OF INVENTION (Disclose details of invention in Part II on reverse)

Michelson Fiber Optic Point Temperature Sensor

RECOMMENDED SECURITY CLASSIFICATION ON INVENTION DISCLOSURE

Unclassified

3. CONCEPTION, INITIAL RECORDS AND RESULTS OF FIRST MODEL

a. EARLIEST DATE AND PLACE INVENTION WAS CONCEIVED (Identify persons and records to support date and place)

Aug. 16, 1982, Office of inventor, T.G.G.

b. DATE AND PRESENT LOCATION OF FIRST SKETCH, DRAWING OR PHOTO AND FIRST WRITTEN DESCRIPTION (Such as notebook entries, etc.)

Memorandum, Aug. 16, 1982 from S.J.P. to T.G.G.

c. DATE AND PLACE OF COMPLETION OF FIRST OPERATING MODEL OR FULL SIZE DEVICE AND ITS PRESENT LOCATION

Sep. 14, 1982 at NRL; currently located at NRL, B12/R205

d. DATE AND PLACE OF FIRST TEST OR OPERATION AND THE RESULTS (Give name and address of witnesses, and present location of records)

Sep. 14, 1982 – records in notebook of inventor, S.J.P. located at NRL, B12/R201

4. OTHER RECORDS (Notebook entries, descriptions, reports, drawings, etc.)

IDENTIFICATION	DATE OF DOCUMENT	PRESENT LOCATION

5. OTHER INDIVIDUALS TO WHOM INVENTION WAS DISCLOSED

NAME	ACTIVITY OR COMPANY INDIVIDUAL REPRESENTS	DATE DISCLOSED	TYPE (Oral or written disclosure)
G. H. Sigel, Jr.	NRL, Optical Techniques Branch	Aug., Sep. 1982	oral
K. P. Koo			
C. A. V. Tarruel			
W. K. Burns			

e. DATE AND PLACE OF OTHER TESTS OR OPERATIONS, AND THE RESULTS (List name and address of witnesses and identify present location of records)

None

Phase sensitivity and linewidth narrowing in a Fox–Smith configured semiconductor laser

S. J. Petuchowski, R. O. Miles, A. Dandridge, and T. G. Giallorenzi
Naval Research Laboratory, Washington, D.C. 20375

(Received 3 November 1981; accepted for publication 24 November 1981)

The behavior and spectral characteristics of a constricted double heterojunction injection laser in a regime in which the lasing characteristics are dominated by a cavity comprised of two external mirrors is reported. The Fox–Smith configuration is shown to limit the lasers emission (previously multimode) to a single longitudinal mode with a linewidth of less than 200 kHz. It is also shown that this laser interferometer configuration is effective as an extended, external cavity laser diode sensor.

PACS numbers: 42.55.Px, 42.60.Da

The sensitivity of the output intensity of a diode laser to both the amplitude and phase of external optical feedback is well documented.[1–4] There has also been substantial interest in the spectral characteristics of the emission under various conditions of external feedback including the introduction of extra-cavity dispersive elements.[5] In this letter, we report operation of a constricted double heterojunction (CDH) injection laser in a regime in which lasing characteristics are dominated by a cavity comprised of two external mirrors configured such that the lasing medium "sees" one constant reflecting surface and one reflector of variable complex amplitude of reflection. The observation of emission linewidth narrowing and the application of this configuration as a sensor are discussed below.

The configurations shown in Fig. 1 are two conformations of the Fox–Smith interferometric cavity employed to achieve single-mode operation of various classes of lasers.[6] Both were implemented by using a CDH diode laser coated to provide high reflectivity at one facet M_1 and a quoted reflectivity of 5% at the opposite lasing facet. The laser was coupled to the external cavity comprised of gold-coated concave mirrors M_2 and M_3 and beam splitter BS ($T = 54\%$, $R = 39\%$ at 0.83 μm) by means of a 45× microscope objective.

The dashed lines in Fig. 1 represent the actual reflectivity r_2 of the laser facet. r_3 represents an effective reflectivity arising from the external cavity reflector elements. The free-running laser with no external feedback ($r_3^2 = 0.05$) exhibited a lasing threshold current of 104 mA with emission over several longitudinal modes. Feedback from just M_2 alone ($r_3^2 \approx 0.15$ assuming an estimated coupling efficiency of 30%) lowered the threshold to 93 mA. We have observed that, both above and below the threshold of the free-standing laser, the introduction of mirror M_3 can constrain oscillation to a single mode, and that the linewidth of the emission is a function of the position of M_3 and is thus controllable.

Since the laser output was observed to depend upon the position of mirror M_3, M_3 was mounted on a piezoelectric translator (PZT) allowing displacement of the mirror over several wavelengths. This also provided a means for periodic modulation of the pathlength. A triangle-wave voltage was used to drive the piezoelectric element corresponding to a peak-to-peak optical path variation of approximately $\pi/2$.

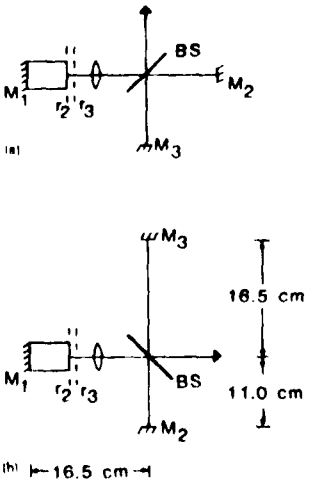

FIG. 1. Fox–Smith type diode laser configurations. Dimensions of the experiment are shown in (b).

 0003-6951/82/040302-03$01.00

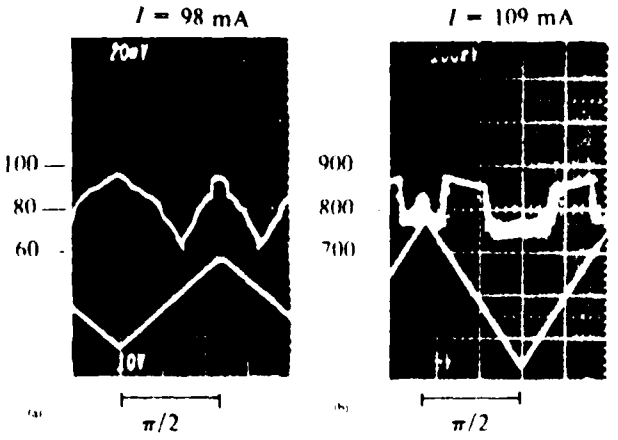

FIG. 2. Laser output vs relative displacement of M_3 in terms of optical phase. (a) Below, (b) above lasing threshold of the free-standing laser. Output units are consistent.

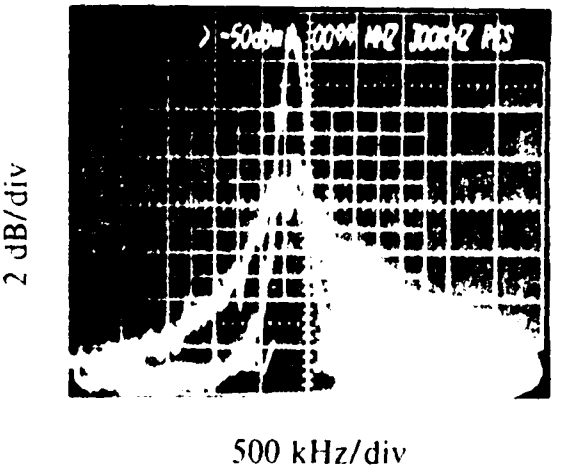

FIG. 3. Spectra of the heterodyne signal at two displacements of M_3, I_f = 107 mA.

For operating currents below the free-running laser threshold, the amplitude of the light output was observed to be a sensitive function of the position of M_3 as shown in Fig. 2(a), with discrete mode jumping clearly evident. For operating currents above the free-running laser threshold, stable single mode operation was observed only over a portion of the mirror excursion. Higher laser output amplitude was obtained under this condition as shown in Fig. 2(b). When the laser operated on a stable single longitudinal mode the output amplitude was high and varied with mirror displacement. Otherwise, the output dropped by approximately 15% and the laser broke into multimode operation exhibiting significantly increased amplitude noise on the order of 10^3 times the minimum noise level. Miles[7] *et al.* observed similar increases of low frequency amplitude noise induced by phase dependent optical feedback in channel substrate planar and buried heterostructure lasers.

Emission linewidth of the external Fox–Smith diode laser was measured by means of a delayed self-heterodyne scheme.[8] A beam splitter divided the output equally into two beams. One beam was frequency shifted by ~90 MHz using an acousto-optic modulator. The second was delayed through an 820-m length of optical fiber.[9] The two beams were then recombined and mixed in an avalanche photodiode. The resolution of this measurement was limited to ~120 kHz by the length of fiber delay line. It was observed that when the Fox–Smith external cavity laser was operating in a stable single mode regime, as shown in Fig. 2(b), the linewidth varied with displacement of M_3 from 150 to 320 kHz as seen in Fig. 3. Linewidths equal to or less than 120 kHz were also observed below the free-running laser threshold in this configuration.

Spectral narrowing in semiconductor laser sources used in interferometric sensor systems reduces frequency instabilities (phase noise) 10 dB or more.[9] Such a reduction in phase noise permits the use of optical path differences (OPD) in the sensor arms ten times longer than in those instances where a free-running laser diode is used as the source. The Fox–Smith external cavity diode laser configuration provides a mechanism to effectively control the emission linewidth. The increased coherence length allows extension of the sensor arm of a diode laser sensor.[10] Alternatively, the Fox–Smith could act as a source for a Mach–Zehnder-type interferometer sensor.[11]

In order to evaluate the sensitivity of such a device the minimum detectable phase variation was measured. The external cavity laser source and detector were mounted in an evacuated isolation chamber to minimize ambient room noise. A dc bias voltage on the PZT of M_3 held the emission to a single longitudinal mode low noise regime. The output, from 50 Hz to 20 kHz was measured with a Tektronix 7 LS spectrum analyzer, while a calibrated modulation voltage was applied to the PZT. Comparison with the noise level over the same frequency range for an operating current of 103 mA yielded the minimum detectable phase variation as a function of frequency shown in Fig. 4. For frequencies greater than 1 kHz microradian level sensitivities were realized, however, the sensor noise increased approximately as $f^{-1/2}$

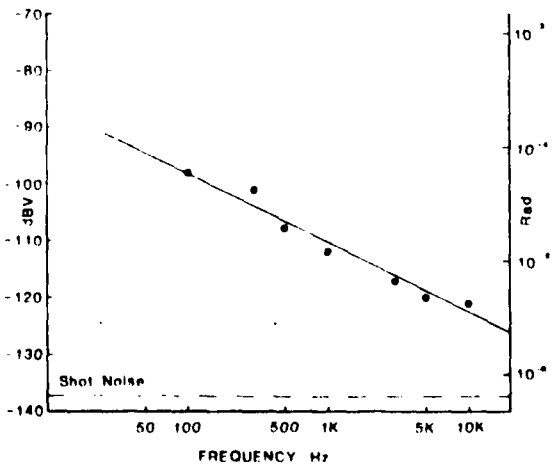

FIG. 4. Fox–Smith sensor noise and corresponding minimum detectable phase modulation. Data normalized to 1-Hz bandwidth referenced to 1-V dc on the detector.

yielding a minimum detectable signal of about 100 μ rad at 100 Hz. When compared to the simple external cavity diode laser sensor[10] the level of performance is found to be nearly two orders of magnitude lower. The dynamic range in the absence of electronic compensation was limited by the response nonlinearity evident in Fig. 2 with harmonic content of the signal never better than -40 dB.

It has been shown previously that both amplitude and phase noise of GaAlAs lasers exhibit an approximate $f^{-1/2}$ behavior.[12,13] In the case of the single reflector diode laser sensor, the short length of the external cavity ($< 10\,\mu$m) ensured that phase noise contributions were negligible. It was also found that the amplitude noise in the single reflector diode laser sensor was about equal to the $f^{-1/2}$ noise in the free-running laser. For the Fox–Smith external cavity configuration, it is not clear whether amplitude or phase noise is the major contribution to the decreased sensitivity. When comparing the Fox–Smith line narrowed configuration to interferometer systems[11] with free-running laser sources, an effective OPD 30 times larger can be used without increase in phase noise. An extension to an all fiber configuration is suggested.

In conclusion, we have shown that a Fox–Smith interferometer configuration when used with a semiconductor laser with one facet antireflection coated, is effective in limiting emission to a single longitudinal mode with a linewidth on the order of 200 kHz or less. We have demonstrated that this laser interferometer configuration is effective as an extended, external laser diode sensor. The increased coherence length of this device makes it attractive as a source for coherent fiber optic communications applications as well as for conventional interferometric sensors.

The authors acknowledge the assistance of L. Goldberg in performing the linewidth measurements and are grateful to him and H. F. Taylor for helpful discussions.

[1] R. P. Salathé, Appl. Phys. **20**, 1 (1979).
[2] R. Lang and K. Kobayashi, IEEE J. Quantum Electron. **QE-16**, 347 (1980).
[3] A. Olsson and C. L. Tang, IEEE J. Quantum Electron. **QE-17**, 1320 (1981).
[4] D. Akerman, P. G. Elisseev, A. Kaiper, M. A. Man'ko, and Z. Roab, Sov. J. Quantum. Electron. **1**, 60 (1971); C. Voumard, R. Salathe, and H. Weber, Appl. Phys. **7**, 123 (1975).
[5] D. Botez, Appl. Phys. Lett. **33**, 872 (1978).
[6] P. W. Smith, IEEE J. Quantum. Electron. **QE-1**, 343 (1965).
[7] R. O. Miles, A. Dandridge, A. B. Tveten, T. G. Giallorenzi, and H. F. Taylor, Appl. Phys. Lett. **38**, 848 (1981).
[8] T. Okoshi, K. Kikuchi, and A. Nakayama, Electron. Lett. **16**, 630 (1980).
[9] L. Goldberg, A. Dandridge, R. O. Miles, T. G. Giallorenzi, and J. F. Weller, *Electron. Lett.* **17**, 677 (1981).
[10] A. Dandridge, R. O. Miles, and T. G. Giallorenzi, Electron. Lett. **16**, 948 (1980).
[11] D. A. Jackson, A. Dandridge, and S. K. Sheem, Opt. Lett. **5**, 139 (1980).
[12] A. Dandridge, A. B. Tveten, R. O. Miles, and T. G. Giallorenzi, Appl. Phys. Lett. **37**, 526 (1980).
[13] A. Dandridge and A. B. Tveten, Appl. Phys. Lett. **39**, 530 (1980).

APPENDIX D

Fabry–Perot photothermal trace detection

A. J. Campillo
U.S. Naval Research Laboratory, Washington, D.C. 20375

S. J. Petuchowski
Phoenix Corporation, McLean, Virginia 22102

Christopher C. Davis
Department of Electrical Engineering, University of Maryland, College Park, Maryland 20742

H-B. Lin
Department of Energy and the Environment, Brookhaven National Laboratory, Upton, New York 11973

(Received 2 April 1982; accepted for publication 8 June 1982)

A novel trace gas detection scheme based upon the photothermal effect following light absorption is described. The resulting index change, which is proportional to the trace species absorption and concentration, is measured interferometrically in a stabilized Fabry–Perot cavity. An experimental noise limit corresponding to an absorption coefficient of 4×10^{-8} cm^{-1}/(Hz$^{1/2}$) was observed. We discuss possible improvements and estimate the ultimate sensitivities achievable with this technique.

PACS numbers: 06.70.Dn, 07.60.Hv, 42.60. – v

Local interrogation of the index of refraction modulation produced in a medium by photoinduced heating constitutes the basis of several photothermal schemes for measuring small absorption. Examples include phase fluctuation optical heterodyne (PFLOH) detection,[1] thermal lensing,[2] and laser beam deflection techniques.[3] The first of these has been proven useful in sensitive trace-gas detection schemes,[4,5] the study of aerosol absorption,[6] and of microwave absorption in liquids,[7] and has been shown to be competitive with photoacoustic (PA) detection.[8] PFLOH detection monitors the refractive index change by placing the heated sample in a Mach–Zehnder interferometer employing a stable single frequency helium neon laser.

We report a new technique in which the refractive index change is also monitored interferometrically but in a Fabry–Perot cavity incorporating the sample medium, thereby enhancing the detection sensitivity over that obtained in PFLOH detection by a factor which depends on the finesse of the cavity. The finesse expresses the ratio of peak spacing to peak full width at half-maximum for the transmitted probe power as a function of optical phase delay per pass. We have demonstrated the feasibility of this scheme in a preliminary experiment in which a calibrated mixture of NO_2 in nitrogen flowed through a Fabry–Perot cavity and its absorption at 514.5 nm was detected.

An experimental noise limit corresponding to an absorption coefficient of 4×10^{-8} cm^{-1}/(Hz$^{1/2}$) was observed. In this letter we discuss possible improvements and estimate the ultimate sensitivities achievable with this technique. It appears that measurement of absorption coefficients less than 10^{-10} cm^{-1} is possible.

As in kindred photothermal detection techniques, energy is deposited and excites the medium by resonant absorption of electromagnetic radiation. Collisional relaxation of the excited mode results in local heating of the background medium and, consequently, to induced local variation in the density of the medium. Detection by transduction of the pressure change is the basis of PA which necessarily involves the integration of signal over the volume from which acoustic or barometric waves impinge on the transducer. The density variation is also manifested in the concomitant change of index of refraction given, in a gas, by the Clausius–Mossotti relation:

$$dn = -(n-1)dT/T_{\rm abs}, \tag{1}$$

where n is the refractive index, $T_{\rm abs}$ is the absolute temperature, and dT is the increment of induced local temperature elevation. Over a pathlength L, this change is tantamount to a variation in optical path or phase delay of

$$d\phi = (2\pi L/\lambda)\,dn, \tag{2}$$

where λ is the wavelength of the probe beam whose heating effect can be neglected.

Our technique is based upon the multipass interferometric measurement of optical path variations in a Fabry–Perot etalon containing the excited medium. Since only the path traversed by the probe beam is interrogated, this technique affords spatial resolution and the application to tomographic flame analysis is suggested.

The fractional transmission of an ideally monochromatic probe beam through the etalon is a periodic function of the optical phase delay per traversal, ϕ:

$$\begin{aligned} &T = T_{\rm max}\, f(\phi) \\ &f(\phi) = (1+\delta\sin^2\phi)^{-1}, \\ &\delta = (F/\pi)^2, \end{aligned} \tag{3}$$

where F is the cavity finesse. Maximum sensitivity of transmission to variations in phase delay occurs at a phase delay of ϕ_0 for which

$$\begin{aligned} \cos(2\phi_0) &= \tfrac{1}{2}(9+4/\delta+4/\delta^2)^{1/2} - 1/\delta - 1/2 \\ &\approx 1 - 2/(3\delta) \quad \text{when } \delta \gg 1. \end{aligned} \tag{4}$$

The trace detection technique entails maintaining the static phase delay at ϕ_0 by means of servo control of the etalon spacing and inducing a periodic phase perturbation, $\phi_m\cos(\omega_m t)$. In the case of $\delta \gg 1$,

 0003-6951/82/040327-03$01.00

$$f(t) \simeq [1 + \tfrac{1}{4}\cos(2\phi_m \cos\omega_m t) + \delta/3 \sin(2\phi_m \cos\omega_m t)]^{-1}. \quad (5)$$

From the small argument limit of the Bessel function expansion, one obtains the Fourier component of the transmitted intensity at the fundamental excitation frequency

$$T^{\omega_m} = [T_{max}(\sqrt{3\delta})/2]\phi_m = (T_{max}\sqrt{3}/\pi)F\phi_m. \quad (6)$$

It is thus evident that the induced signal, in the linear limit, is directly proportional to the finesse. The attraction of this technique is the smaller sample path required for comparable sensitivity to that afforded by the Mach–Zehnder PFLOH configuration.

This advantage is translated into increased detection sensitivity only to the extent that the source of limiting noise is not similarly enhanced. Of the contributions to system noise, phase noise of the probe source laser (deviation from monochromicity), mechanical noise inducing either a cavity $\langle \Delta L \rangle$ or beam misalignment, and window effects due to periodic heating of the etalon plates scale with finesse, as does the signal. Amplitude noise on the source beam can, in principle, be compensated, and detector shot noise depends solely on net power incident on the detector and scales with $T_{max}^{1/2}$.

The experiment was implemented as depicted schematically in Fig. 1. A single-frequency He-Ne laser (Tropel 200) was used as the interferometer source. The Fabry–Perot cavity was a Burleigh RC-110 with an etalon spacing of 12 cm. The mirrors, one flat and one concave ($R = 6$ m), were dielectric coated for high reflectivity at 633 nm, and a finesse of 50 could be achieved. Optical isolation of the reflected beam and phase matching of the beam into the etalon were accomplished by the polarizer/retarder combination and lens L, respectively. Aperture A was inserted in the cavity to inhibit higher order transverse cavity modes.

Absorption was detected in a flowing calibrated mixture of 99 ppm NO_2 in nitrogen. The excitation source was the continuous wave beam of an argon ion laser chopped with a mechanical chopping wheel. This 514.5-nm beam was coupled into the Fabry–Perot cavity at a slight angle from the normal so as to minimize dependence of the intracavity excitation density on etalon spacing. Filter F blocked the green beam from detection by the photomultiplier PM and no signal was present in the absence of the He-Ne probe beam.

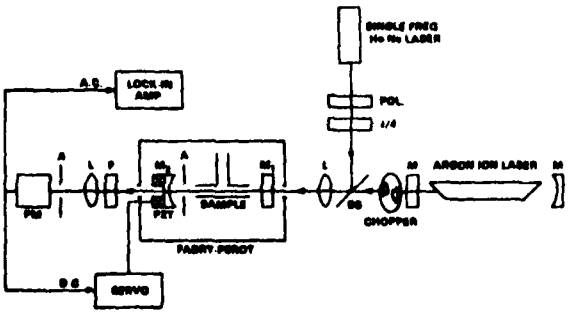

FIG. 1. Experimental configuration. BS—beam splitter, L—lens, M_1, M_2—Fabry–Perot mirrors, F—633-nm bandpass filter, and PM—photomultiplier tube.

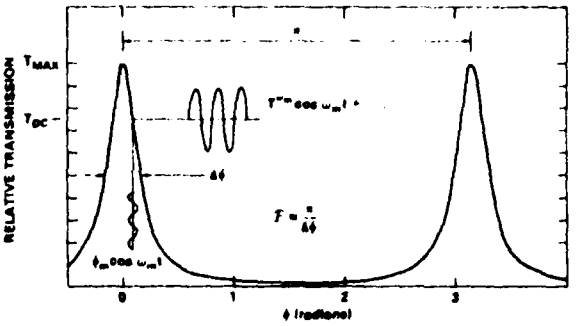

FIG. 2. Calculated Fabry–Perot tranamission function for a finesse $F = 15$.

The sample flowed, at a rate of 0.2 l/min, through a windowless cell consisting of a 10-cm-long by 3-mm-diam bore glass tube with a central gas inlet mounted centrally in the Fabry–Perot cavity. Both beams were approximately $TEM_{(0)}$ and nearly coaxial with the cell, and focused to beam waists (radius at half-field strength) at M_1 of 0.38 and 0.2 mm for the excitation and probe beams, respectively. In order to maintain the etalon at a spacing corresponding to the optical phase delay of maximum sensitivity in the face of slow thermal drift due to cumulative heating, the difference between the photomultiplier load voltage and a fixed reference voltage was amplified, integrated, and fed back to a piezoelectric element to translate one of the etalon plates. Noise spectra were measured using a Tektronix 7L5 spectrum analyzer.

The heating of a cylindrical gas sample by a Gaussian beam has been studied by Davis and Petuchowski.[5] In the current experiment, the condition of $b \gg \omega_e$, where b is the container radius and ω_e is the beam parameter of the excitation beam, was not rigorously satisfied. Thus the heating along the axis in the region interrogated by the probe is probably somewhat less efficient at low frequencies than would otherwise be the case. At a chopping frequency of 400 Hz, the modulation period is short compared to the thermal diffusion time across the sample in air at 1 atm, and, on axis,

$$T \simeq I_0\alpha/(2C_p\omega_m)\sin(\omega_m t), \quad (7)$$

where I_0 is the peak excitation power density, α is the absorption coefficient of the sample, and C_p is the specific heat at constant pressure.

Inserting Eq. (7) into earlier expressions for index and optical phase and evaluating, for atmospheric pressure nitrogen, $n - 1 = 2.92 \times 10^{-4}$, $C_p = 1.17 \times 10^{-3}$ cal/cm^3, $T_{abs} = 300$ °K, $\omega_m = 2\pi \times 400$ s^{-1}, $L = 10$ cm, $\lambda = 633$ nm, one calculates $\Delta\phi_m/(I_0\alpha) = 0.17$ rad cm^3/W.

For 99 ppm NO_2 ($\alpha = 6 \times 10^{-4}$ cm^{-1}) (Ref. 9) in 1 atm N_2, the phase modulation amplitude due to excitation at 400 Hz with 30-mW average power ($I_0 = 26$ W/cm^2) is calculated to be 2.7 mrad. The observed signal is shown against the background noise spectrum in Fig. 3. The ordinate is normalized to the dc voltage corresponding to maximum transmission indicating a signal of -40 dB or 1.0% modulation. At a finesse of 50, Eq. (6) implies an expected signal of 7.3% or -22.7 dB.

The lower sensitivity actually observed is attributed to

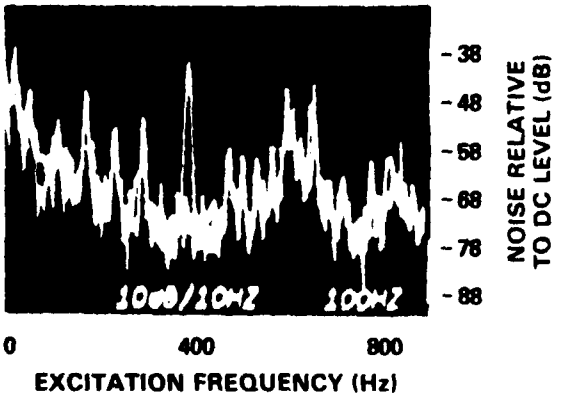

FIG. 3. Interferometer noise level, showing signal at 400 Hz due to 99 ppm NO_2 in nitrogen with 30-mW excitation at 514.5 nm.

operation at other than the optimal phase point and possible finesse degradation during the course of the experiment.

The noise floor at 400 Hz shown in Fig. 3 corresponds to a minimum detectable absorption (1-Hz detection bandwidth) of 1.3×10^{-7} cm^{-1} W (or 7 ppb NO_2 with 3-W excitation). Actual sensitivity was limited by a residual signal of -55.7 dB present even when the cell was continuously flushed with pure N_2. This limitation is attributed to synchronous heating of the optics and the adjacent air layers by the excitation beam, and could be overcome by coupling the excitation beams into the cavity transversely to the probe.

In order to estimate ultimate sensitivity limitations of the technique, we note that the noise floor ($\Delta f = 1$ Hz) of -83 dBV observed at 400 Hz is due to mechanical noise, $\langle \Delta L \rangle / L$, to which the cavity is as sensitive as to signal. Careful design of a stable etalon, deliberate choice of operating frequency at an acoustic null, and electronic subtraction of source amplitude noise should allow operation limited by shot noise, for our source, at -132 dBV. Density fluctuations in the sample will not limit sensitivity for samples at atmospheric pressure even of dimensions on the order of the He-Ne beam waist.

Shot noise limited detection with a cavity finesse of 50 corresponds to a phase sensitivity of 9×10^{-9} rad/($\sqrt{\text{Hz}}$). Considering the extreme stability required, this might be achievable only in sealed environments or condensed phase samples. A more reasonable phase sensitivity of 10^{-7} rad/($\sqrt{\text{Hz}}$) in our system with $L = 1$ cm corresponds to an absorption sensitivity of 1.9×10^{-10} cm^{-1} W.

We have demonstrated a simple interferometric technique for performing photothermal spectroscopy of transparent media with extreme sensitivity and spatial resolution.

[1] C. C. Davis, Appl. Phys. Lett. **36**, 515 (1980).
[2] J. P. Gordon, R. C. C. Leite, R. S. Moore, S. P. S. Porto, and J. R. Whinnery, J. Appl. Phys. **36**, 3 (1965).
[3] J. C. Murphy and L. C. Aamodt, J. Appl. Phys. **51**, 4580 (1980).
[4] A. J. Campillo, H-B. Lin, C. J. Dodge, and C. C. Davis, Opt. Lett. **5**, 424 (1980).
[5] C. C. Davis and S. J. Petuchowski, Appl. Opt. **20**, 2539 (1981).
[6] A. J. Campillo and H-B. Lin, SPIE Proc. **286**, 24 (1981).
[7] M. L. Swicord and C. C. Davis, Radio Sci. (in press).
[8] *Optoacoustic Spectroscopy and Detection*, edited by Y. H. Pao (Academic, New York, 1977).
[9] R. W. Terhune and J. E. Anderson, Opt. Lett. **1**, 70 (1977).

APPENDIX E

FIBER OPTIC THERMAL SENSORS

S. J. Petuchowski
Phoenix Corporation

Gregory S. Maurer and Luise Schuetz
Naval Research Laboratory

Theoretical calculations suggest that optical fibers can perform thermometry with unprecedented sensitivity and frequency response. The high sensitivity results from the strong temperature dependence of the effective optical path length in the fiber, and the wide frequency response from the extremely low thermal mass of the fiber. Additional advantages of these sensors include the ability to operate in electromagnetically active environments and the ability to optically integrate thermal variations over finite distances. The performance of fiber optic thermal sensors is the subject of an active research effort at NRL.

Experimental verification of the thermal response was accomplished by coating sample fibers with an aluminum jacket. The fibers were then heated by passing AC current through the jacket.[1,2] Thermally induced phase shifts were detected using Mach - Zehnder interferometry. Two single-mode fibers and one multimode fiber were studied; the thickness of the aluminum jackets ranged from 1.2 μm to 20 μm. The magnitude of the temperature variations was calculated from known experimental parameters and a simplistic cooling model, and was confirmed in one instance using a Chromel-Constantan thermocouple.

Dynamic thermal response was observed from 1 Hz to 30 kHz, although resonances above 3 kHz preclude a simple analysis of the frequency response.

These resonances are ascribed to mechanical resonances in the fiber, and appear to be related to the specific fiber configuration. Minimum detectable temperatures for a 1 cm length of fiber, assuming a minimum detectable phase shift of 10^{-6} radians, are 10 μK for the 1.2 micrc jacket and 1μK for the 20 micron jacket.

The ability of the fiber to spatially integrate thermal fluctuations was verified by imposing a low-frequency square wave current through one section of a sample fiber and a high-frequency sine wave through another section. As expected, the optical output of the fiber was the superposition of the individual waveforms.

An analytic model has been developed for the dynamic thermal response of multilayered optical fibers.[3] This model calculates the phase of coherent light passing through the fiber as a function of the fiber surface temperature. The effects included in the model are 1) thermally induced changes in fiber length, 2) the temperature dependence of the refractive index, and 3) changes in refractive index resulting from thermally induced strains in the fibers.

The model has been run for the single-mode fiber and agrees quite well with measured results. Discrepancies are attributed to incomplete knowledge of the fiber surface temperature and of the thermoelastic parameters of the fiber. The model can be used with confidence to predict the performance of various fiber designs and several designs will be discussed with regard to the optimization of the sensor for different temperature-sensing applications.

REFERENCES

1. Gregory S. Maurer, J. H. Cole, and J. A. Bucaro, "Sensitive, High-Speed Thermometry Using Optical Fibers," accepted for publication in Optics Letters.

2. S. J. Petuchowski, G. H. Sigel, Jr., and T. G. Giallorenzi, "Single Mode Fibre Point and Extended Temperature Sensors" ~~submitted to~~ to be published in Electronics Letters.

3. Luise S. Schuetz, J. H. Cole, J. Jarzynski, N. Lagakos, and J. A. Bucaro, "Dynamic Thermal Response of Single Mode Optical Fiber for Interferometric Sensors," submitted to Applied Optics.

SINGLE-MODE-FIBRE POINT AND EXTENDED TEMPERATURE SENSORS

Indexing terms: *Optical fibres, Optical sensors, Temperature measurement*

The response of single-mode fibres to time-varying thermal perturbations has been characterised by using a Mach-Zehnder interferometer. It is shown that single-mode fibres offer the possibility of high-speed, high-sensitivity remote temperature sensing with a minimum disturbance of the thermal environment and the capability to operate in an electromagnetically active environment. In addition, fibre temperature sensors can be configured to measure not only the specific temperature at any given point, but also offer the unique feature of extended temperature measurements over the length of a fibre segment in which the device optically integrates any thermally induced fluctuations.

Optical-fibre sensor technology has advanced rapidly during the past few years.[1] A key sensor area which has received only minor attention thus far is that of temperature monitoring. The steady-state response of fibres to temperature has been measured[2-5] and a preliminary demonstration of optical phase sensitivity to an AC heating current was reported by Dandridge *et al.*[6] A qualitative study of the response of a fibre interferometer to impulse heating has recently been reported by Musha and Katsumoto.[7] In this letter we report a quantitative study of the sensitivity of a fibre-optic temperature sensor and a demonstration of its operation in a spatially integrating mode.

The greatest potential for this class of sensors lies in their use as high-speed, very high-sensitivity remote thermal measurement devices. Dielectric fibre temperature sensors can operate in electromagnetically active environments without difficulty, and their small volume and heat capacity produces a minimum perturbation of the thermal environment being measured. Such applications as the *in situ* spatially resolved analysis of temperature distributions in flames appear promising.

This letter describes the sensitivity and frequency response of single-mode fibres incorporated in one arm of a Mach-Zehnder interferometer using the same basic configurations described previously.[1] The interferometer was composed entirely of single-mode optical fibre (ITT, 5 μm core diameter) with an optical path difference between the arms of $\sim$ 2 cm to permit homodyne demodulation using a phase generated carrier scheme[8] at signal frequencies above 50 Hz and ordinary static interferometric operation below 50 Hz. One arm was stripped of its polymer jacketing and coated by evaporation with aluminium to a thickness of $\sim$ 1·2 μm. The coating was evaporated in segments of length $\sim$ 2·5 cm, separated by masked sections of bare fibre of comparable length. Spring-brass contacts held the sensor arm in contact with a plastic base and permitted separately controlled electrical currents to flow through the coatings of each of the segments. The sensor configuration is shown in Fig. 1. In order to demonstrate the capability of the fibre to integrate temperature variations along its length, current waveforms of different shapes and frequencies were applied simultaneously to separate sensor segments, and total phase response was measured.

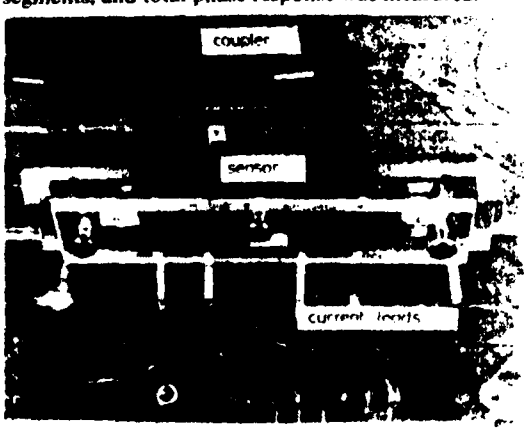

The dynamic temperature response of the surface of the coated fibre to ohmic heating is governed by diffusion of heat into the fibre as well as heat loss at the surface due to conduction of heat to the brass contacts, plastic base and thermocouple leads, natural convection currents set up in the surrounding air, and black-body radiation from the surface. We note that only the diffusion of heat into the fibre is germane to the response of the sensor to variations in the temperature of the surrounding heat bath. Calculation of the sensor response requires solution of the heat diffusion boundary value problem[9] for the concentric cylindrical regions of core, cladding and coating, and subsequent solution for the induced strains so as to derive optical phase response. We have performed an empirical study of the frequency response.

In order to calibrate the periodic surface heating in response to a sinusoidal current through the aluminium coating, it was necessary to consider heat loss to the environment. The time scale for heat diffusion into the fibre, considering it as a uniform silica cylinder, is in the order of $a^2/\kappa \approx 3{\cdot}1 \times 10^{-3}$ s, where $a = 43$ μm is the fibre radius and $\kappa = 5{\cdot}8 \times 10^{-3}$ cm^2/s is the thermal diffusivity of fused silica. By comparison, the rise time to thermal equilibrium in air was found to be in the order of seconds.

The ohmic heating of the fibre surface, typically in the order of millidegrees Kelvin, was estimated by means of a thermocouple (Omega, CO2-E) of 0·5 mm Chromel Constantan foil, in mechanical contact with the upper surface of the fibre, midway between the brass contacts. The temperature response to heating current actually measured was that of the thermocouple junction, and a finite temperature gradient is to be expected even in the steady state. The rise time of the thermocouple free standing in air was measured by heating with a helium-neon laser beam to be 50 ± 5 ms, and dynamic temperature measurements were corrected accordingly.

Absolute temperature calibration was performed according to the following: we assume the measured temperature T_m to be linearly related by a coefficient β to the actual temperature elevation of the fibre surface T. We adopt a simplistic picture in which the fibre is considered as an infinite cylinder of effective thermal mass C per unit length, and all heat loss mechanisms are lumped into a linear coefficient H. Thus,

$$dT/dt = C^{-1}(I^2R - HT) \tag{1}$$

where I is the heating current, and R is the resistance per unit length of the coating. From the solution for time independent current,

$$T = \frac{I^2R}{H}(1 - e^{-Ht/C}) \tag{2}$$

it is clear that the observed quadratic current dependence of the steady-state temperature, as measured with the thermocouple, over the range of heating currents (< 100 mA) applied in the experiment, indicates that H is independent of temperature to within experimental accuracy. The measured slope of steady-state temperature T_m against I^2R yields $H/\beta = 3{\cdot}6$ mW/cm deg for the calibrated sensor segment, and the measured rise time to steady state of 0·96 s allows the solution for $C/\beta = 3{\cdot}5$ mJ/cm deg.

A comparison of rise times in air at atmospheric pressure and at reduced pressures down to $\sim$ 1 torr showed that the dominant heat-loss mechanism in the configuration described is due to conductive heat sinking by the brass contacts and base. The effective thermal mass derived in this manner compares with a calculated value, assuming homogeneous fused silica, of 0·11 mJ/cm deg. Thus, measured temperatures are corrected by a factor $\beta = 0{\cdot}031$.

The dynamic temperature response to periodic heating was determined by plotting the response at the first harmonic to a sinusoidal current about zero offset, and, as expected from a substitution of $I = I_0 \sin wt$ in eqn. 1, is approximately inversely proportional to frequency at frequencies above 1 Hz.

The actual response of the fibre-optic temperature sensor to heating with a constant RMS current is plotted against frequency in Fig. 2a. The skin effect [illegible] negligible over the fre-

kHz, and these are attributed to mechanical resonances of the fibre. The response, as plotted in Fig. 2b, has been normalised for the f^{-1} heating behaviour of the surface, and thus reflects absolute sensor response against temperature. The DC response values of Lagakos *et al.*[4] are shown for comparison. It is apparent that the frequency response, after correction for the expected f^{-1} dependence, varies by no more than a factor of 5.5 from 3 Hz to the first resonance, above 3 kHz. The origin of the actual response curve remains to be explained by analysing the effect of coating properties. The possibility that the unexpected rolloff in response below 100 Hz is due entirely to interferometer nonlinearity is discounted by the measurements below 10 Hz performed at lower levels of heating current.

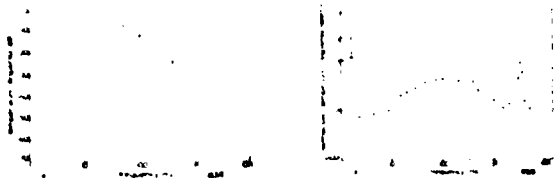

Fig. 2

a Temperature response against frequency
RMS heating current is 67 (6.7) mA above (below) 10 Hz. Circles are for passively stabilised interferometer
b Normalised temperature response against frequency
DC values from Reference 4: 1. Jacketed fibre; 2. Bare fibre

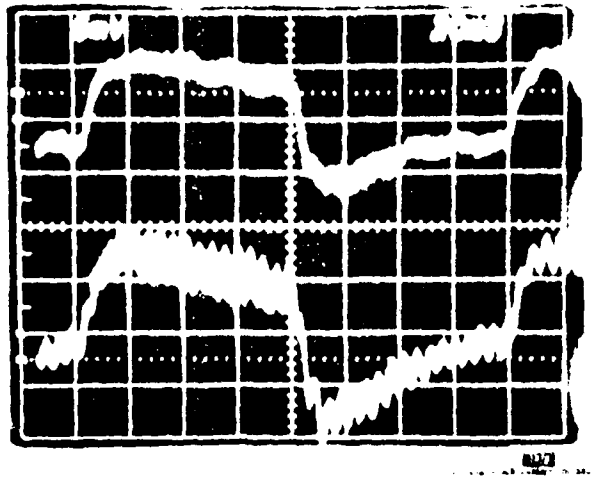

Fig. 3 *Single (upper trace) and dual (lower trace) segment heating*

Fig. 3 illustrates the integrating capabilities of the fibre-optic temperature sensor; a unipolar square-wave current of 6.3 mA at 6.5 Hz was applied to one sensor segment in both traces, while in the lower trace a sinusoidal current of 21 mA RMS at 106 Hz was applied to a second segment in the same sensor arm. The resultant interferometer signal shows the sum of the two heating effects.

In summary, the sensitivity and frequency response of single-mode-fibre temperature sensors has been measured using an all-fibre interferometer, and the advantages of the device have been outlined. Perhaps the most interesting feature of the fibre thermal sensors is their ability to optically integrate signals generated by thermal fluctuations at spatially separated locations, thereby eliminating the need for a large number of point sensors.

S. J. PETUCHOWSKI
G. H. SIGEL
T. G. GIALLORENZI
Naval Research Laboratory
Washington, DC 20375, USA

3rd August 1982

COLE, J. H., BANSETTOR, S. C., and PRIEST, R. G.: 'Optical fiber sensor technology', *IEEE J. Quantum Electron.*, 1982, **QE-18**, p. 626
2 BUCKER, G. B.: 'Fiber optic sensing of pressure', *Appl. Opt.*, 1979, **19**, p. 1445
3 HYUMA, K., TAI, S., SAWADA, T., and SUSOSHITA, M.: 'Fibre-optic instrument for temperature measurement', *IEEE J. Quantum Electron.*, 1982, **QE-18**, p. 676
4 LAGAKOS, N., BUCARO, J. A., and JARZYNSKI, J.: 'Temperature-induced optical phase shifts in fibers', *Appl. Opt.*, 1981, **20**, p. 2305
5 YOSHINO, T., and OHNO, Y.: 'Fiber Fabry Perot interferometers' Presented at International Conference on integrated optics and optical fiber communication, San Francisco, CA, April 1981, paper WL2
6 DANDRIDGE, A., TVETEN, A. B., and GIALLORENZI, T. G.: 'Interferometric current sensors using optical fibres', *Electron. Lett.*, 1981, **17**, pp. 523–525
7 MUSHA, T., and KATSUMOTO, T.: 'Phase oscillation in fiber interferometer caused by light impulse', *Jpn. J. Appl. Phys.*, 1982, **21**, p. L275
8 DANDRIDGE, A., TVETEN, A. B., and GIALLORENZI, T. G.: 'Homodyne demodulation scheme for fiber optic sensors using phase generated carrier', *IEEE J. Quantum Electron.*, to be published
9 CARSLAW, H. S., and JAEGER, J. C.: 'Conduction of heat in solids' (Oxford University Press, 1959)

0013-5194/82/190814-02$1.50/0

LOW-LOSS LANGE COUPLER

Indexing terms: Microwave circuits and systems, Couplers

The use of air-bridge straps in place of bond wires on the Lange coupler on an alumina substrate is investigated. It is shown that the resultant coupler has lower loss when compared with a coupler using bond wires and is more suitable for mass production than the bond-wire type.

Introduction: The use of the Lange coupler to make hybrid 3 dB couplers is well established. However, in order to equalise the odd- and even-mode phase velocities, bond wires have to be used to join alternate lines of the coupler. In monolithic circuits the incorporation of bond wires is not possible. Thus, techniques have been developed by which the bond wires have been replaced by air bridges.[1,2] However, no comparison is known to have been made of the loss associated with air-bridge and wire-bonded couplers on alumina.

Using similar techniques, as for monolithic circuits, Lange couplers have been fabricated on alumina substrates. The results of measurements on such couplers have been compared with identical couplers constructed with bond wires. The comparison shows that up to 0.5 dB lower loss may be expected at 18 GHz as a result of using air-bridge straps.

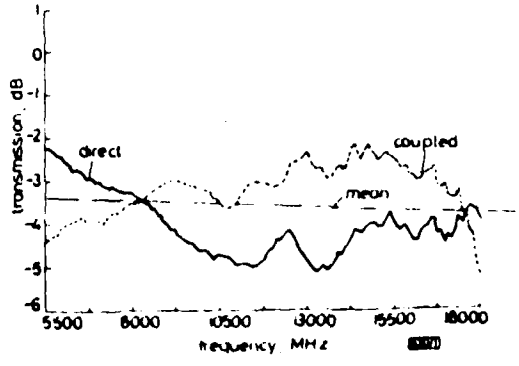

Fig. 4 *Transmission for Lange coupler with air-bridge straps*

Guide to Use of the HP-9836 for Real-Time Data Acquisition and Control of the HP-3582A Spectrum Analyzer

Note: Suggested modifications to the program are delimited $$$like this$$$.

I. SUMMARY

The program, "FFT_SETUP" allows the HP-9836 desktop computer to task the HP-2240A Measurement and Control Processor (MCP) to acquire real-time signals over extended periods of time (up to seven hours) and to perform manipulation and display of the acquired data in the temporal and frequency domains, by using the dedicated fast-Fourier-transform (FFT) capabilities of the HP-3582A Fourier-Transform Spectrum Analyzer. This software is intended as a building block and to illustrate the capabilities of the aforementioned instruments to be operated in concert for the control and data-processing connected with very low frequency (VLF) experiments. In particular, it allows extension of the spectrum analysis capability of the 3582A to a resolution of 145 microHertz.

II. GENERAL GUIDE TO USE OF THE PROGRAM

A. Loading the Program

...operating System (OS)

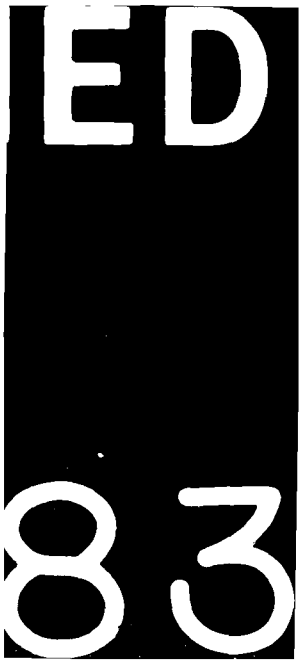
ED
83